SUPPRESSING EFFECT OF VARIOUS MINERAL ADMIXTURES ON COMBINED DETERIORATION CAUSED BY ASR AND CHLORIDE ATTACK

Chikao Sannoh[1,*], Kazuyuki Torii[2]

[1]Hokuriku Electric Power Company, 15-1 Ushijima-machi, TOYAMA, Japan

[2]Kanazawa University, Kakuma-machi, KANAZAWA, Japan

Abstract

This study aims at investigating the effect of various mineral admixtures in controlling the combined deterioration caused by ASR and chloride attack. In this study, four types of mineral admixtures were prepared. The fly ashes were originally produced in the Hokuriku district. RC specimens with reactive river sand and reactive river gravel in the Hokuriku district were exposed on the seashore at the Shinminato harbor in Toyama prefecture. The outdoor exposure test in the saline environment has started in September 2004, where both the expansion behavior of concrete and steel corrosion characteristics were periodically measured. As a result, it has been shown that ASR is controlled effectively by the use of various mineral admixtures, and that the expansion of concrete with reactive river sand and reactive river gravel due to ASR is controlled by the replacement of 15% fly ash which is categorized according to JIS A6201 as class Ⅱ or by the replacement of 40% ground granulated blast furnace slag which is categorized according to JIS A6206 as class 4000,and the replacement ratio is consistent with the recommendation according to JIS A5308.

Keywords: Alkali-silica reaction, Mineral admixtures, Chloride attack, Combined deterioration mechanisms, Outdoor exposure test

1 INTRODUCTION

As one of the suppression measures against the alkali-silica reaction (referred to as ASR, hereafter), the methods to use blended cement with ASR suppression effects are stipulated in JIS A5308 (Appendix 2). On the other hand, in this provision, a method to control the total alkali quantity in the concrete is stipulated. However, under the severe saline environment, where alkali such as NaCl is supplied to concrete from the external environment (for instance, seawater in an oceanic environment or anti-freezing agents), the sole regulation of the total alkali is not sufficient, and more positive measures using mineral admixtures are expected to become urgent[1].

In order to examine the ASR suppression effects of various types of mineral admixtures, the authors have been conducting comparative examinations, under various accelerated curing conditions, on the ASR expansion behavior of mortar and concrete specimens using mineral admixtures[2,3]. The various accelerated curing tests (JIS A1146, Denmark method, and ASTM C1260) used in evaluating ASR suppression effects based on mineral admixtures are methods to judge the alkali-silica reactivity of aggregates. Although testing methods to judge the pozzolanic reactivity of fly ash have been proposed up to now, standards for evaluating the ASR suppression effects of mineral admixtures have not been stipulated. ASTM C1567 has been proposed as standard test method for evaluating suppressing effects of mineral admixtures on ASR.(ASTM C1567-07 Standard Test Method for Determing the Potential Alkali-Silica Reactivity of Combinations of Cementitious Materials and Aggregate (Accelerated Mortar-Bar Method)) For this reason, it is considered important to confirm ASR suppression effects in actual constructions, to clarify the correlation with indoor acceleration tests, and to indicate the standards for evaluation in an indoor acceleration test, in terms of the future expansion of application of mineral admixtures in ASR suppression measures.

This study aimed to evaluate the suppression effects of the concrete using various types of mineral admixtures (fly ash, blast furnace slag powder, green tuff powder, and roofing tile powder) against combined deterioration action caused by ASR and chloride attack, and conducted experimental examinations on the expansion behavior and corrosion conditions of large-sized RC specimens under an oceanic exposure environment.

* Correspondence to: sannoh.chikao@rikuden.co.jp

2 MATERIALS AND METHODS

2.1 Materials

The physical and chemical properties of two types of river sands and river gravels each from different river systems (Joganji River and Hayatsuki River in Toyama Prefecture) are shown in Table 1. As reactive aggregates, the river sand and river gravel produced in the Joganji River, which were confirmed to have ASR damage in actual constructions, were used. The river sand and river gravel produced in the Joganji River contains approximately 30% of andesite (reactive components: cristobalite and volcanic glass). In addition, as non-reactive aggregates, the river sand and river gravel produced in the Hayatsuki River (containing granite and diorite) were used. As cement, ordinary Portland cement (density: 3.16 g/cm3, specific surface area: 3330 cm2/g, alkali content: 0.68%) was used. The physical properties and chemical components of mineral admixtures used in this study (fly ash (FA), blast furnace slag powder (BFS), green tuff powder (ZO), and roofing tile powder (RP)) are shown in Table 2

The fly ash was produced at a coal-burning power plant of the Hokuriku District (Nanao-ohta Power Station in Ishikawa Prefecture), and its quality conformed to JIS A6201 type II ash. Blast furnace slag powder was blast furnace slag powder 4000 that was standardized in JIS A6206. Green tuff powder was produced in Mikuni-cho, Fukui Prefecture, and it was used after being pulverized to 8 μm of average diameter using a hummer mill after natural drying. Roofing tile powder was the crushed material (10 mm or below) manufactured at a roofing tile waste crushing plant under operation in Fukui Prefecture, and it was used after sieving with a 75 μm sieve. The mix proportion of concrete is shown in Table 3. The replacement of various types of admixtures was subject to an inner ratio of replacement (percent in total 100%), and the replacement ratio of FA was set at 15% stipulated in the ASR suppression measures of JIS A5308, and the replacement ratio of ZO and RP was set at the same ratio as FA. The replacement ratio of BFS was set at 40%. Concrete was plain concrete without adding chemical admixtures, and the concrete doped with alkali was prepared by adding 10 kg/m3 Na2Oeq using NaCl.

The X-ray diffraction charts of various types of mineral admixtures are shown in Fig. 1. In FA, there is a halo (broad peaks of 2θ=15-35°) that shows the presence of a glass phase, as well as the peaks of a quartz phase (α-SiO2) and a mullite phase (3SiO2·2Al2O3) as crystalline minerals. Since BFS powder does not show a clear peak other than the merillite phase, it is judged to be amorphous.

2.2 Methods

The outline of an RC specimen (500 x 500 x 200 mm) is shown in Fig. 2. The cover concrete of rebar (SD295A, rebar diameter: vertical reinforcement of φ19 mm and transverse reinforcement of φ16 mm) was set at 20 mm. The combination of additives and aggregates of the specimens is shown in Table 4 (sole cement is indicated as OPC). RC specimens were exposed, after two weeks of curing, on the quay of the Shinminato harbor in Toyama Prefecture, where the effect of floating salt was large, in September 2004 (refer to Photo. 1). Measurement of expansion rate of the concrete and electrochemical monitoring (half-cell potential and polarization resistance) of reinforcing rebar were periodically conducted. In measurement of expansion rate, contact chips (base length: 100 mm) were fixed on the RC specimen, and a contact gauge was used for measurement. Electrochemical monitoring was performed by measuring half-cell potential and polarization resistance with a portable reinforcing rebar corrosion tester (SRI-CM-III, reference electrode: silver/saturated silver chloride electrode). The relational expression of Stern-Geary between corrosion rate and polarization resistance is shown in the formula (1).

$$Icorr = K/Rp \quad (1)$$

Where: Icorr: Corrosion rate (μA/cm2)
Rp: Polarization resistance (Ωcm2)
K: Constant based on the type of metals, environment etc. (mV)

As K value, K=26 (mV), which was obtained by Andrade et al. [4], was used in this study.

3 RESULTS AND DISCUSSIONS

3.1 External Observation of RC Specimens

The changed external view of an RC specimen after 20 months (May 2006) of exposure is shown in Fig. 3. In Specimens 1 and 2, after one month of exposure, corrosion cracking (0.05 mm) along the outer circumferential reinforcing steel was found. In addition, in Specimen 2, minute popping-out was observed on the surface. During the first winter (December-March,2005), large

external changes were not observed. When the exposure reached 6-9 months (March-June), cracking along the internal reinforcing steel was observed, and the cracking width increased as a whole. After 10 months of exposure (July 2005), rust fluid was generated from the crack (cracking width of 0.2 mm) of Specimen 1. In Specimen 2, hexagonal patterns of crack caused by ASR came to be prominently observed.

Regarding specimens blended with mineral admixtures, Specimens 6, 10, 14 and 18 were prepared using non-innocuous aggregates doped with NaCl. After 12 months of exposure, these specimens generated a crack (to a width of 0.1-0.2 mm) along the reinforcing steel, and after 18 months of exposure, cracking width increased (cracking width of 0.3-0.4 mm). However, hexagonal patterns of the crack observed in Specimen 2 hardly appeared. On the other hand, Specimens 5, 9, 13 and 17, which were prepared using innocuous aggregates, suffered cracking along the reinforcing steel, but its degree was suppressed compared with Specimens 6, 10, 14 and 18. The reason why specimens using non-innocuous aggregates suffered fast cracking was considered as follows: (1) ASR was encouraged near the reinforcing steel due to water supply from the crack of the reinforcing steel corrosion, or (2) the reinforcing steel corrosion was encouraged due to minute ASR cracking. After 18 months of exposure, minute peeling generated on the crack of reinforcing steel, and coarse reinforcing steel was observed under the peeling surface (refer to Photo. 2). These results revealed that even if mineral admixtures were added, when a high concentration of initial salt was inherent, corrosion proceeded, and ASR also proceeded if water was supplied. Regarding the difference of pozzolanic materials, the cracking suppression performance was in the order of BFS > FA > RP > ZO. On the other hand, specimens without added NaCl did not show external changes even after 20 months (May 2006) of exposure.

3.2 Expansion Behavior of the Concrete

The measurement results of the expansion rate of RC specimens (containing reactive aggregates) are shown in Fig. 4. Regarding a single ingredient of cement (OPC), specimens doped with NaCl expanded at relatively early stages, different from those without added NaCl. Even though the expansion rate was slow in the first winter (December-March,2005), the expansion became large during 6-9 months (March-June) of exposure, resulting in more than a 0.15% expansion. In specimens blended with mineral admixtures, although early expansion was observed when NaCl was added, the expansion was suppressed later to around half the case of a single ingredient of cement. On the other hand, the expansion suppression effects were depending on the types of mineral admixtures, and the expansion of specimens doped with NaCl was smaller in the order of BFS < FA < RP < ZO. This order is consistent with the changes of appearance.

As described above, the river sand and river gravel of the Joganji river system contains approximately 30% of andesite containing cristobalite and volcanic glass as reactive minerals. It is well known that the aggregates produced in the rivers of the Hokuriku district contain reactive aggregates such as andesite, rhyolite and chert, and that the contents of these materials substantially vary from one river system to another river system. Since the river sand and river gravel used in this test is thought to have a mixing rate near the pessimum value, these aggregates are considered to have the highest reactivity within river-made aggregates in the Hokuriku district. This experiment has demonstrated that high-quality mineral admixtures such as BFS and FA at the replacement rate stipulated in JIS A5308 suppress ASR of concrete incorporated with aggregates produced in the rivers of Toyama Prefecture.

3.3 Electrochemical Monitoring of Steel Corrosion

(1) Half-cell Potential

The measurement results of the half-cell potential of RC specimens are shown in Figs. 5-8. When we followed the judgment criteria of ASTM C876-91, independently of the types of aggregates, the measured values of the half-cell potential of RC specimens without adding NaCl at one month of exposure, when measured values were stabilized, were larger than –90 mV, which was in the range of "non-corrosion state with the probability of 90% or above." When NaCl was added, the figures were –230 mV or below, which was in the range of "corrosion state with the probability of 90% or above." This fact indicates that passive state of steel materials in the specimens doped with NaCl had already been destroyed and steel was in unstable conditions. The specimens doped with NaCl suffered change in half-cell potential moving to a less-noble side since the summer of the first year of exposure independently of the types of aggregates and mineral admixtures, which showed that the corrosion of steel materials was actively advancing.

On the other hand, when NaCl was not added, natural potential slightly transferred to the less-noble side since the summer of the first year. It is thought for the penetration of exogenous salt components, but the effects of the exogenous salts were trivial in the first year of exposure in whole. Within these specimens, only Specimen 3 (OPC: use of innocuous aggregate) suffered change in natural potential moving to the less-noble side, which suggested existence of the effects of exogenous salts. Compared with this material, Specimen 4 (OPC: use of non-innocuous aggregate) maintained the noble side of natural potential. A paper reported a case that in a mortar containing a reactive aggregate, the corrosion of steel material was suppressed due to the formation of a uniform alkaline silica gel layer surrounding the steel material[5]. In Specimen 4 (OPC: use of non-innocuous aggregate), such phenomenon may have occurred. Regarding the difference of mineral admixture materials, the half-cell potential of BFS (Specimen 9 and 10) tended to be at the noble side compared with other mineral admixtures.

(2) Corrosion Rate

The measurement results of the corrosion rate of RC specimens are shown in Figs. 9-12. Regarding the corrosion rate, according to the judgment criteria of CEB, below 0.1 μA/cm2 is evaluated as "of passive state", 0.1-1 μA/cm2 as "contingent," and 1 μA/cm2 or above as "of high corrosion rate." The half-cell potential agreed mostly with trend of corrosion rate. However, the corrosion rate is strongly affected by the atmospheric temperature, and the activation period and the stagnation period of the steel material corrosion repeate through the year. Specimen 1, in which rust liquid was generated from the crack, prominently increased the corrosion rate after 18-20 months (March-May) of exposure. Regarding the difference of mineral admixtures, within specimens doped with NaCl, the corrosion rate of RP and ZO (Specimen 13, 14 and 18) tended to be high. These specimens showed a prominently high generation rate of cracking in appearance, showing the accordance between external changes and the measurement results. Regarding specimens without adding NaCl, specimens with mineral admixtures all showed small a corrosion rate compared with OPC. This phenomenon suggests that through the addition of mineral admixtures, salt component penetration has been suppressed over a long period of time.

3.4 Effects of Various Types of Mineral Material Admixtures on Combined Deterioration Due to ASR and Chloride Attack

The deterioration factors common to ASR and chloride attack, there are the supply of water and the intrusion of sodium chloride. As a mechanism of NaCl to encourage ASR, two phenomena were reported: (1) due to the intrusion of NaCl, hydroxide ions in the concrete increase, and (2) chloride ions themselves encourage an alkali silica reaction[6]. Regarding the corrosion of reinforcing steel, the passive state is destroyed, and corrosion proceeds due to the supply of oxygen and water. In this experiment, through the addition of mineral admixtures, the expansion rate of specimens doped with NaCl was suppressed to approximately half that of OPC, and the crack of hexagonal patterns specific to ASR was hardly observed. However, cracking along the reinforcing steel was generated, and this crack was severer than that of specimens using an innocuous aggregate. This fact suggested, as described above, that ASR was encouraged from water supplied from cracking generated from salt damage, or that reinforcing steel corrosion was encouraged due to minute cracking of ASR, and that further combined deterioration proceeded because of these two reasons. One of the reasons why mineral admixtures bring about ASR suppression effect is the densification of concrete structure. However, it has been found that when water is supplied due to the generation of cracking, ASR proceeds. It has also been found that when there are high concentrations of initial salt components, even adding mineral admixtures cannot suppress corrosion.

4 CONCLUSIONS

The results of this study can be summarized as follows:

(1) In outdoor exposure experiments under the addition of various types of mineral admixtures, suppression effects against ASR expansion were demonstrated.

(2) For the ASR suppression measure using river-made aggregates in Toyama Prefecture, it has been demonstrated that the use of good-quality mineral admixtures such as blast furnace slag powder or fly ash at the replacement ratio stipulated in JIS A5308 can effectively suppress ASR.

(3) When there are initial salt components, even with added mineral admixtures, corrosion cracking occurs, which progreses to combined deterioration, where ASR also proceeds due to the supply of water from the crack.

(4) Electrochemical measurement has enabled monitoring of the corrosion conditions of RC specimens suffering from ASR deterioration.

5 REFERENCES

[1] Nixon,P.,Hawthorn,F.,Sims,I. : Developing an International Specification to Combat AAR Proposals of RILEM TC 191-ARP,Proceedings of the 12th International Conference on Alkali-Aggregate Reaction in Concrete,Volume1,pp.8-16(2004)

[2] Sannoh,C.,Torii,K.,Yamato,H.,Noguchi,Y. : Effect of Pozzolanic Additives produced in Hokuriku District on Alkali-Silica Expansion of Mortars,Cement Science and Concrete Technology,No.58,pp.233-240(2004)

[3] Sannoh,C.,Torii,K.,Saitoh,T.,Tomotake,H. : Evaluation of Alkali-Silica Reactivity of Concrete using various Pozzolanic Additives, Cement Science and Concrete Technology,No.59,pp.317-324(2005)

[4] Andrade,C.,Gonzalez,J. : Quantitative Measurements of Corrosion Rate of Reinforcing Steels Embedded in Concrete Using Polarization Resistance Measurements , Werkstoffe und Korrosion,Vol.29, pp.515-519(1978)

[5] Kawamura,M.,Singhal,M.,Tuji,Y. : Effect of ASR on Corrosion of Reinforcement in Concrete under Saline Environment,Proc.of East-Asia Alkali-Aggregate Reaction Seminar,Tottori,pp.179-190(1997)

[6] Kawamura,M.,Takemoto,K.,Terashima,N. : Effect of sodium chloride and sodium hydroxide from the surrounding solution on alkali-silica reaction in mortars containing fly ash, Magazine of Concrete Research,Vol.40,No.144,pp.143-151(1988)

Photo. 1: External view of exposure site.

Photo. 2: View of scaling on concrete.

TABLE 1: Physical and chemical properties of aggregates used in this study.

	Joganji river		Hayatsuki river	
	River sand	River gravel	River sand	River gravel
Maximum size(mm)	5	20	5	20
Density in saturated surface-dry condition(g/m^3)	2.62	2.64	2.63	2.68
Density in oven-dry condition(g/m^3)	2.58	2.61	2.59	2.66
Percentage of absorption(%)	1.7	1.3	1.5	0.8
ASR Reactivity of aggregate	Not Innocuous *1		Innocuous *2	

*1 Mortar-bar method（JIS A 1146） *2 Chemical method（JIS A 1145）

TABLE 2: Physical properties and chemical compositions of mineral admixtures.

Marks	Density (g/cm^3)	Blaine fineness (cm^2/g)	Chemical compositions（Wt.%）									
			ig.loss	SiO_2	Al_2O_3	CaO	Fe_2O_3	MgO	TiO_2	SO_3	Na_2O	K_2O
FA	2.33	3550	1.50	59.6	26.5	0.80	4.89	0.61	1.50	0.36	0.24	1.39
BFS	2.90	4010	0.31	33.1	14.7	42.5	-	5.60	0.58	1.98	0.26	0.26
ZO	1.16	15176*	13.0	61.7	14.7	1.44	2.52	0.60	0.43	-	2.13	3.35
RP	2.61	5300	0	71.2	18.8	0.20	5.16	0.82	0.85	0	0.30	2.55

*BET Specific fineness

TABLE 3: Mix proportion of concrete.

Marks	Gmax (mm)	W/C (%)	s/a (%)	Replacement ratio (%)	Unit content(kg/m^3)				
					Water	Cement	Mineral admixture	River sand	River gravel
OPC	20	50	40	-	175	350	-	749	1106
FA				15		297.5	52.5	721	1086
BFS				40		210	140	721	1086
ZO				15		297.5	52.5	697	1050
RP								724	1090

TABLE 4: Combinations of binder and aggregate.

Specimens number	Additives	NaCl	Aggregate
1	OPC	with	Non-reactive
2			Reactive
3		without	Non-reactive
4			Reactive
5	FA	with	Non-reactive
6			Reactive
7		without	Non-reactive
8			Reactive
9	BFS	with	Non-reactive
10			Reactive
11		without	Non-reactive
12			Reactive
13	ZO	with	Non-reactive
14			Reactive
15		without	Non-reactive
16			Reactive
17	RP	with	Non-reactive
18			Reactive
19		without	Non-reactive
20			Reactive

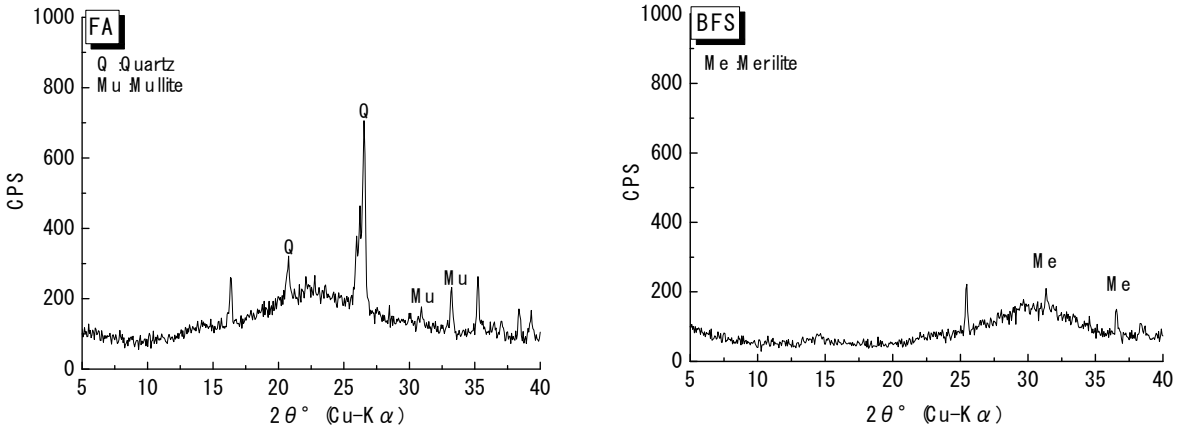

Figure 1: X-ray diffraction patterns of mineral admixtures used in this study.

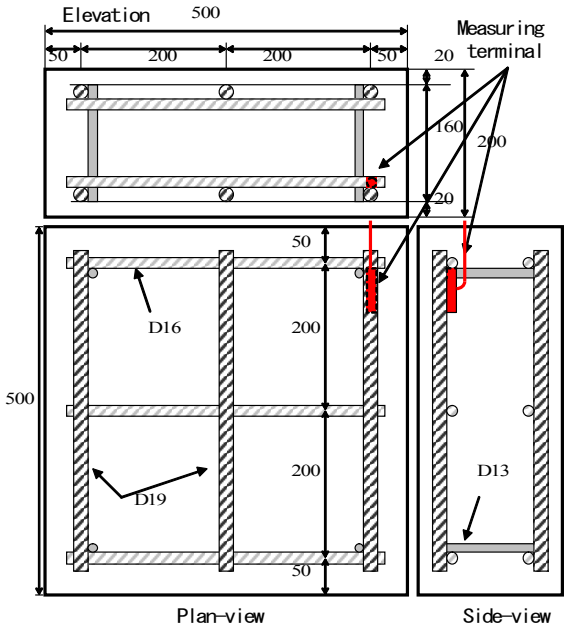

Figure 2: Details of RC specimen.

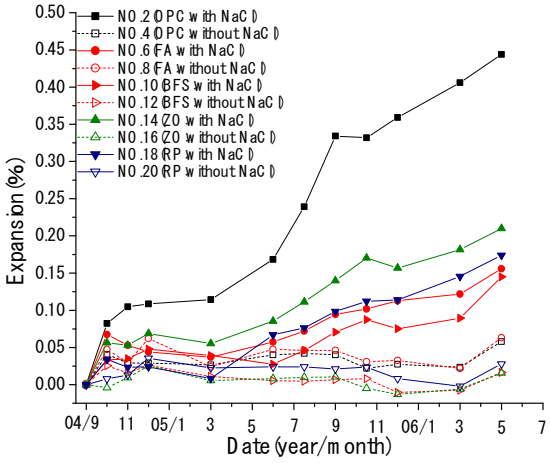

Figure 4: Expansion behavior of RC specimens with and without pozzolanic additives.

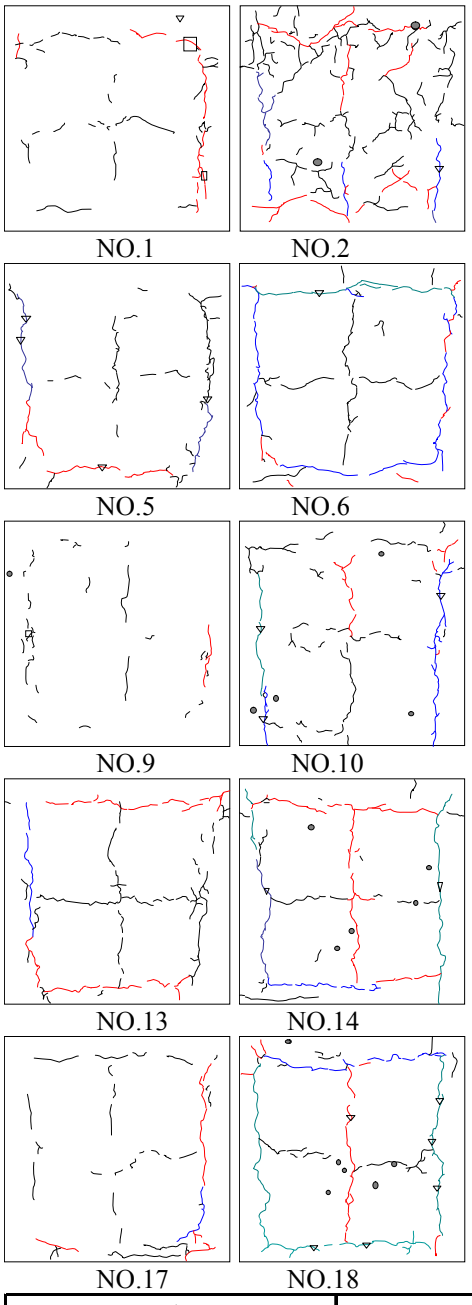

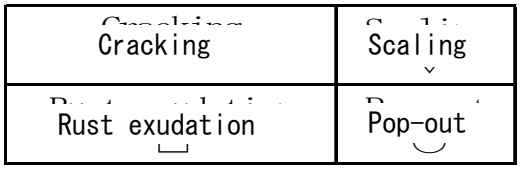

Figure 3: Deterioration map of RC specimens.

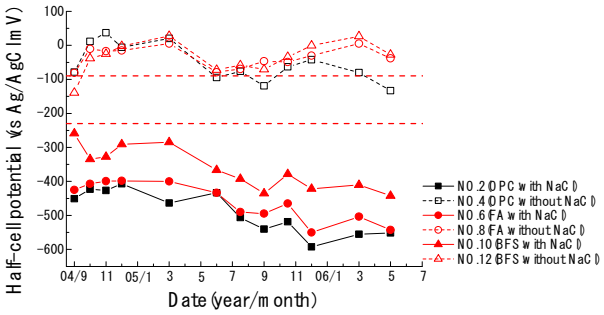

Figure 5: Half-cell potential of RC specimens with reactive aggregate(OPC,FA,BFS).

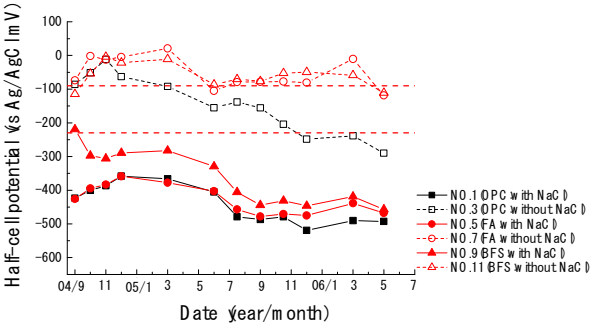

Figure 6: Half-cell potential of RC specimens with non-reactive aggregate(OPC,FA,BFS).

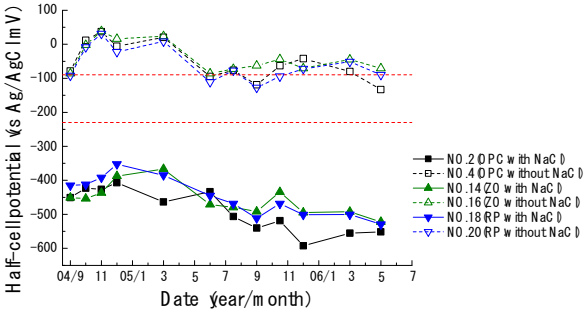

Figure 7: Half-cell potential of RC specimens with reactive aggregate (OPC,ZO,RP).

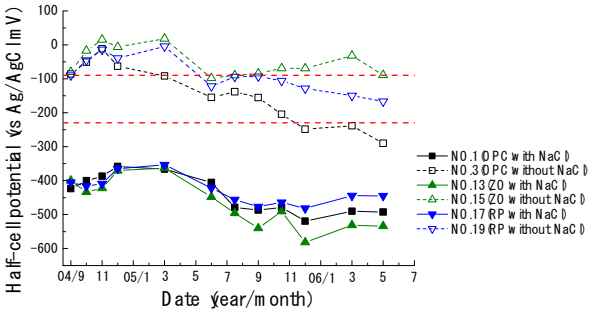

Figure 8: Half-cell potential of RC specimens with non-reactive aggregate (OPC,ZO,RP).

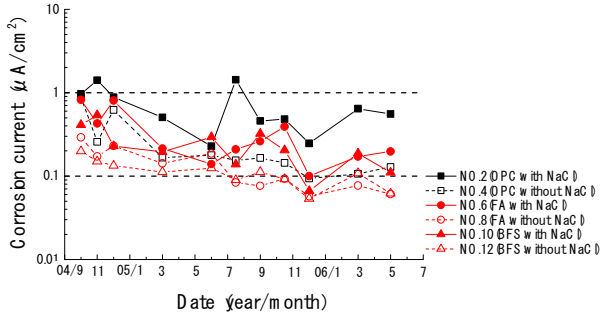

Figure 9: Corrosion current of RC specimens with reactive aggregate(OPC,FA,BFS).

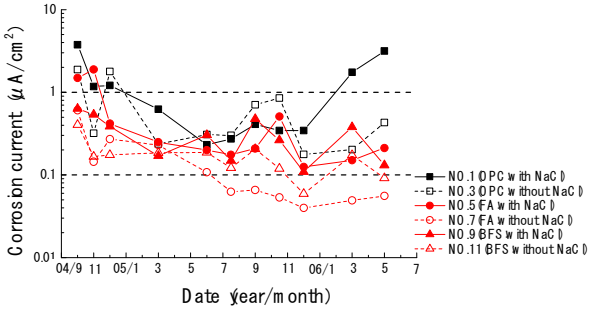

Figure 10: Corrosion current of RC specimens with non-reactive aggregate(OPC,FA,BFS).

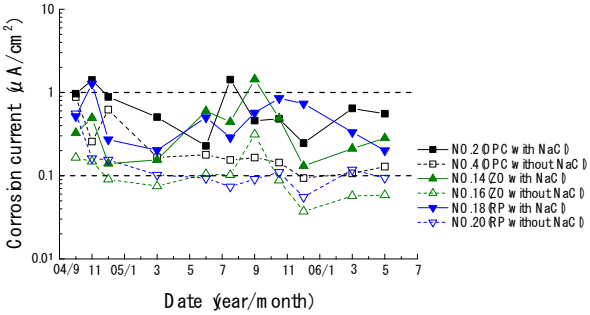

Figure 11: Corrosion current of RC specimens with reactive aggregate (OPC,ZO,RP).

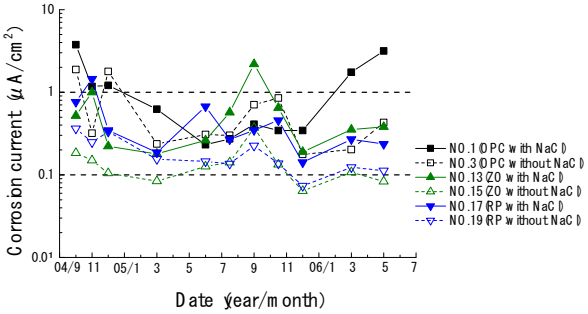

Figure 12: Corrosion current of RC specimens with non-reactive aggregate (OPC,ZO,RP).